ELSEVIER

Organic Electronics 3 (2002) 1–7

Organic Electronics

www.elsevier.com/locate/orgel

Organic monolayers with uniform domain orientation and reduced antiphase boundaries – MBE of perylene on Au(1 1 0)

L. Gross *, C. Seidel, H. Fuchs

Physikalisches Institut, Universität Münster, D-48149 Münster, Germany

Received 18 May 2001; received in revised form 10 September 2001; accepted 10 September 2001

Abstract

The growth of epitaxial monolayers of perylene on Au(1 1 0) was investigated by means of scanning tunneling microscopy (STM) and low energy electron diffraction (LEED). The preparation was done by molecular beam epitaxy (MBE). The experimental setup allowed us to perform LEED or STM measurements during evaporation. The pattern of the adsorbed perylene molecules shows several dosage-induced structural transitions, leading to a final coincident monolayer structure with uniform domain orientation and a low density of antiphase boundaries. The underlying Au(1 1 0) interface exhibits several different reconstructions, depending on the perylene coverage.

PACS: 68.35.R; 34.30; 61.16.C; 61.14.H
Keywords: Au(1 1 0); Perylene; Surface phase transition; STM; LEED; OMBE

1. Introduction

Perylene is a promising semiconductor material for organic electronic devices. Recently, Batlogg et al. presented an organic field-effect transistor (OFET) based on crystalline perylene grown from the vapor phase, which showed electron mobilities as high as 5.5 $cm^2/V\,s$ at room temperature [1]. This is the highest electron mobility in an OFET that has ever been observed, rendering perylene a most promising material for organic electronic devices. For organic materials the charge transport and luminescence properties strongly depend on the structural properties of the thin films [2–4]. Additionally, electronic devices built of highly ordered and oriented films are expected to have special properties, e.g. to emit linearly polarized recombination luminescence in the case of OLEDs. Schäfer et al. showed that single domain oriented multilayers of the perylene derivative 2,9-dimethyl-antra[2,l,9-def:6,5,10-d′e′f]diisoquinoline-l,3,8,10-tetrone (DMe-PTCDI) on Ag(1 1 0) emit linearly polarized fluorescence [5].

Our aim was to prepare highly ordered films using molecular beam epitaxy (MBE). We chose molecules as well as substrates with the same symmetry, 2pmm, which in principle allows single

* Corresponding author. Tel.: +49-251-833-3657; fax: +49-251-833-3602.
E-mail address: grosl@uni-muenster.de (L. Gross).

1566-1199/02/$ - see front matter
PII: S1566-1199(01)00023-4

domain oriented growth, namely when the symmetry axes of the molecules and of the substrate align parallel. Single domain oriented monolayers have been realized for some organic systems already [6–8]. However, there are still distortions by antiphase boundaries. The next systematic step for improving the degree of order of the monolayers would therefore be the reduction of antiphase domain boundaries. The investigated system shows single domain growth which does not start from individual, independent two-dimensional crystalline islands, and therefore can lead to a reduced density of antiphase domain boundaries in the monolayer. It is not only of fundamental importance to study this topic since highly ordered films are also of great importance for technical applications. While the structures of perylene on Au(1 1 0) have been described in a previous paper [9], this paper focuses on the investigation of a special kind of structural transition that can lead to a reduction of antiphase domain boundaries.

2. Experimental

All experiments were performed under ultra-high vacuum (UHV) conditions. The base pressure of the UHV chambers was 1×10^{-8} Pa. Crystal preparation consisted in several cycles of sputtering with Ar^+ ions (500 eV, 6 μA/cm^2, 20 min) and heating up to 700 K for a few minutes. The sample cleanliness was checked by low energy electron diffraction (LEED), X-ray photoemission spectroscopy (XPS) and scanning tunneling microscopy (STM).

Perylene was obtained from [10] and purified by sublimation. Evaporation was done with a Knudsen cells [11] at a temperatures of about 370 K. Sublimation rates and purity were checked by a mass spectrometer (BALZERS QMG 511). The MBE-LEED [12] allowed us to perform LEED measurements during the vapor deposition process and to monitor the structural growth process. For accurate determination of the final monolayer structure an OMICRON spot profile analysis LEED (SPA-LEED) was used. STM measurements were done with an OMICRON variable temperature-STM; electrochemically etched tungsten wires were used as tips. The images shown are unfiltered, but background subtracted. All images were recorded in the constant current mode at 300 K to show height topographies. An extra Knudsen cell made it possible to deposit molecules during STM measurements. The sublimation rates used were such as to form about 0.2 ML (monolayers, ML) deposition per minute.

3. Results

Fig. 1 shows a series of LEED images recorded with the MBE-LEED system during evaporation, beginning with approximately 0.1 ML coverage and ending with a complete, compressed monolayer ($\Theta \equiv 1$ ML). For quantification of the perylene coverage, the XPS of the Cls signal was analyzed at different coverages. In the STM measurements of submonolayer coverages the molecules were usually imaged with reversed contrast (Fig. 2(a) and (b)).

In the submonolayer regime the perylene molecules form chains along the Au-[1 $\bar{1}$ 0] direction with a typical length of 2–10 nm. The chains of molecules are located with their center on top of the Au reconstruction lines (Fig. 2(b)) and show a minimum interchain spacing of $4a_2$ in the [0 0 1] direction, but are otherwise randomly distributed across the surface. The molecules are very mobile in this configuration; in successive STM measurements (recording time 5 min/image) the chains almost always changed adsorption positions. The distance of neighboring molecules in a chain is 1.10–1.19 nm in the Au-[1 $\bar{1}$ 0] direction [9]. At a coverage of about 0.4 ML nearly the whole surface is evenly covered with the [1 $\bar{1}$ 0]-directed perylene rows, with a spacing of $4a_2$ in Au-[0 0 1] direction (Fig. 2(c)). This phase will be referred to as $4a_2$ structure and is the least dense monolayer structure. With increasing coverage the $(0\,1)_{ads.}$ (ads.: adsorbate) spot moves from a $4a_2$ to a $3a_2$ periodicity, as can be seen in the MBE-LEED experiments (Fig. 1(d) and (e)). This corresponds to the spacing of the chains of molecules, in the $3a_2$ structure (i.e. a $3a_2$ spacing of the [1 $\bar{1}$ 0]-directed perylene rows in [0 0 1] direction). At a coverage of $\Theta = 0.6$ ML the whole surface is covered with the

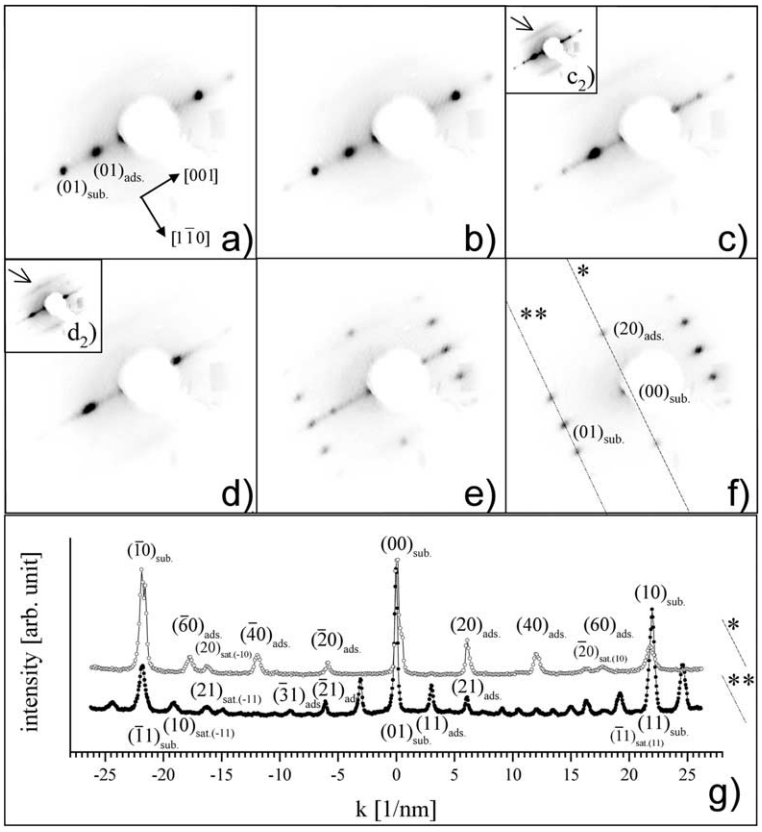

Fig. 1. Series of MBE-LEED measurements of perylene on Au(1 1 0) (inverted, $E = 12.9$ eV), with increasing coverage from $\Theta = 0.1$ ML in (a) to a compressed monolayer ($\theta = 1$ ML) in (f). In some images, the order of the spots corresponding to the adsorbate (ads.) or substrate (sub.) is indicated. In the insets in (c) and (d) the contrast has been enhanced to make the diffuse-linear $(1\,0)_{ads.}$ spots visible. (g) Shows two line profiles, recorded with the SPA-LEED. The coverage and structure is the same as in (f), in which the scanned lines are indicated (* and **). The index sat. refers to satellite reflexes.

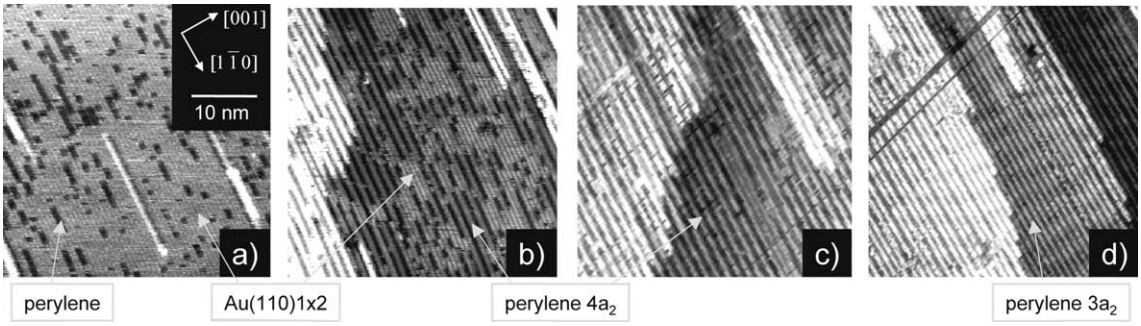

Fig. 2. Series of STM images ($U = 1.0$ V; $I = 0.2$ nA); molecules have been vapor deposited in situ. For a better comparison all images show areas of the same size on the same substrate orientation, for this tilted cutouts of larger scan areas are used in (c) and (d) and the lines seen under approximately 45° are scan lines. In (a) and (b) the [1 1̄ 0]-rows of the uncovered parts of the Au(1 1 0) 1×2 surface can be seen. The molecules appear with reversed contrast (i.e. as dark features) on the Au surface.

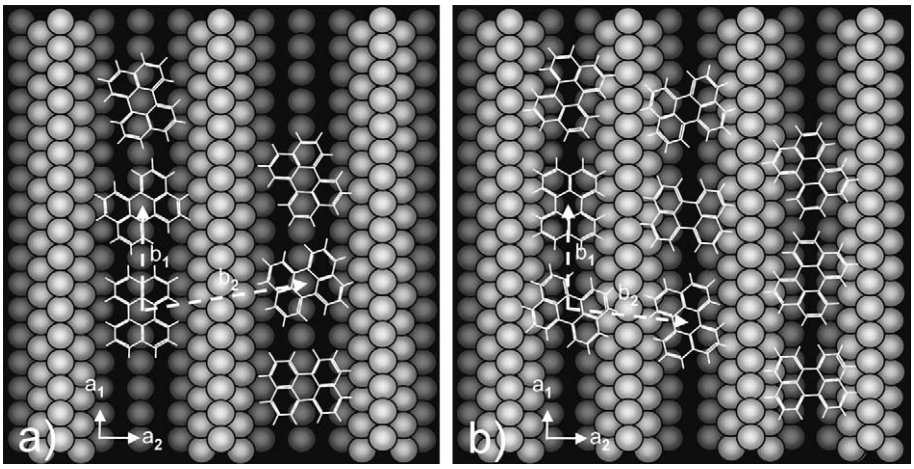

Fig. 3. Proposed real space structure models for the submonolayer structures of perylene on Au(1 1 0): (a) $4a_2$ periodic structure; (b) $3a_2$ periodic structure.

$3a_2$ structure. At this coverage the $(0\,1)_{\text{sub.}}$ (sub.: substrate) spot, corresponding to the (1×2) Au reconstruction, was suppressed at all electron energies used in the LEED investigation (Fig. 1(d)). This indicates that the Au(1 1 0) interface changed its reconstruction. Real space models are shown in Fig. 3 for both of these structures ($4a_2$ and $3a_2$). It should be noted that these structures do not have crystalline order. The adsorption positions in adjacent rows are not correlated, which is the reason for the diffuse-linear $(1\,0)_{\text{ads.}}$ spots in the LEED patterns (Fig. 1c_2 and d_2). The compression from $4a_2$ to $3a_2$ periodicity can also be observed by STM measurements, when further molecules are vapor deposited in situ (Fig. 2(c) and (d)).

The final structure ($\Theta \equiv 1$ ML) shows a sharp LEED pattern in both dimensions (Fig. 1(f)) and has a $2a_2$ periodicity in the $[1\,\bar{1}\,0]$ direction. The unit cell contains two molecules, which are observable as the new $(1\,1)_{\text{ads.}}$ spot occurs (Fig. 1(e)). The $(1\,0)_{\text{ads.}}$ spot is suppressed due to glide plane symmetry. The final monolayer is structure is coincident and can be described by the matrix

$$\text{Perylene}\begin{pmatrix} 7.5 & 0 \\ 0 & 2 \end{pmatrix}\text{Au}(1\,1\,0)$$

Line profiles, recorded with a SPA-LEED (Fig. 1(g)), have been used to determine the coefficients of the matrix with an absolute error of ± 0.1. The unit cell is orthogonal ($\Gamma = 90°$). The unit vector lengths are $b_1 = 2.16(2)$ nm and $b_2 = 0.82(2)$ nm, with b_1 parallel to a_1 ($\Phi = 0°$). The unit cell area is 1.77 nm^2, which is only 89% of the space needed for two plane lying molecules, a finding which suggesting that the molecules are tilted towards the surface normal. The two molecules of the unit cell are probably tilted in different directions, which leads to a bimolecular unit cell. It follows from the suppression of the $(1\,0)_{\text{ads.}}$ spot in the LEED patterns that the tilting of the molecules has to conform to (0 0 1) glide plane symmetry. A real space model is proposed in Fig. 4(b).

From the STM images a very good ordering of the final monolayer can be concluded. We observed only very few domain boundaries. One reason is the single domain orientation, but also only few antiphase domain boundaries are observed. Even at step edges the adsorption spots of the molecules on different terrasses are aligned (Fig. 5(a)).

In STM measurements of the final compressed monolayer only one specific form of antiphase boundaries was observed. In these, the neighboring domains are shifted by half a unit vector in the Au-$[1\,\bar{1}\,0]$ direction, leading to a boundary in which the molecules are still aligned. In contrast to the defect-free monolayer, molecules of inequivalent and in equivalent positions are neighboring along the $[1\,\bar{1}\,0]$ and [0 0 1] directed boundaries,

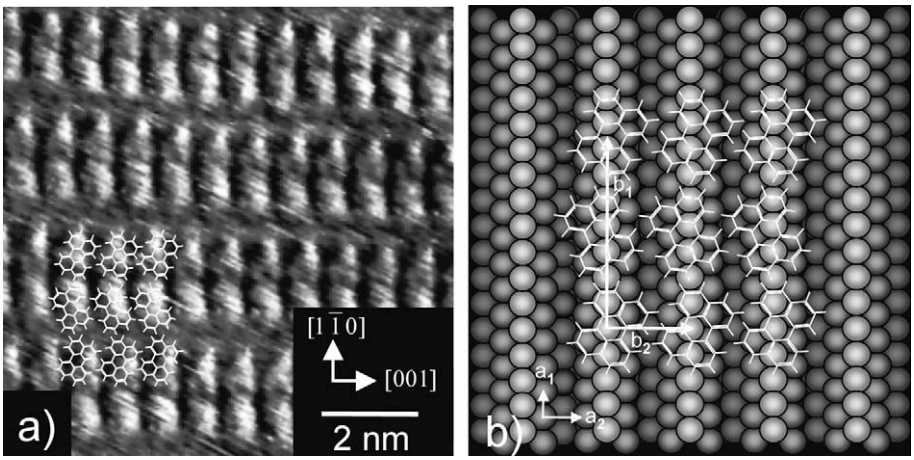

Fig. 4. Compressed monolayer structure: (a) STM measurement ($U = 1.0$ V; $I = 0.2$ nA), molecular structures are drawn into the image; (b) structure model.

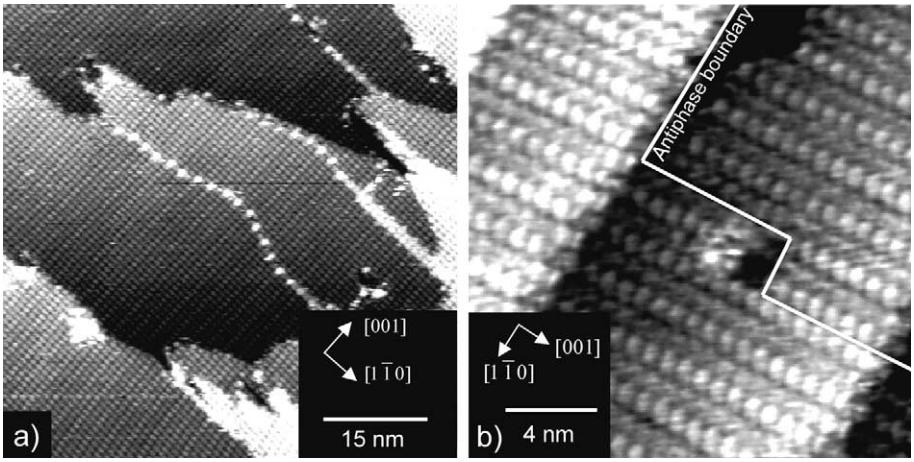

Fig. 5. STM measurements ($U = 1.0$ V; $I = 0.1$ nA) of the compressed monolayer: (a) (69 nm × 69 nm); (b) (20 nm × 20 nm) with an antiphase domain boundary indicated.

respectively (the terms equivalent and inequivalent refer to the two different sites of the unit cell). An antiphase domain boundary of this kind is shown in Fig. 5(b). As can be seen, the boundary runs along a Au step edge in the [1 $\bar{1}$ 0] direction and then in the [0 0 1] direction along a defect. The alignment of the perylene molecules over the step edge can also be seen. Along the antiphase boundary at the step edge molecules of inequivalent positions, which have different brightness in the STM measurement, are neighboring.

4. Discussion

Perylene forms three monolayer structures of different density that are compressed with increasing coverage of the surface. In all structures, the perylene molecules are aligned along the [1 $\bar{1}$ 0] rows of the reconstructed Au(1 1 0) surface. Starting from low perylene coverage the originally 1×2 reconstructed Au surface changes its reconstruction to 1×4 (at $\Theta = 0.4$ ML). With increasing coverage, the periodicity of the Au rows

decreases to 1×3 (at $\Theta = 0.6$ ML) and finally reaches 1×2 again (at $\Theta = 1$ ML). It is already known from calculations of the free Au(1 1 0) surface that $1 \times N$ missing row reconstructions are energetically favored, not only for $N = 2$ but also for higher integer values of N [13]. Such reconstructions of the Au(1 1 0) surface have also been observed in experiments. For example a 1×3 reconstruction at higher temperatures [14,15] and 1×3 and 1×5 reconstructions after annealing in oxygen [16]. Our experiments show that in the case of a coverage with perylene the Au(1 1 0) reconstruction is governed by the degree of coverage.

An image reversal occurs in the case of the perylene submonolayers, in most experiments; the cause of this phenomenon was not investigated in depth. Böhringer et al. observed an image reversal for perylene-tetracarboxylic-dianhydride (PTCDA) on Ag(1 1 0) at room temperature and low tunneling resistance, and explained it with one (or several) trapped molecule(s) between tip and sample [17]. Since the perylene molecules are very mobile at room temperature, the same reason may account for our case.

A comparison of perylene and the derivative DMe-PTCDI [18] on Au(1 1 0) shows a completely different growth mode. DMe-PTCDI grows from nuclei and forms crystalline islands in the submonolayer regime. This growth from crystalline islands is typical also for the well characterized perylene derivative PTCDA on various single crystalline noble metal surfaces, e.g. on Au(1 0 0) [19] or Ag(1 1 0) [17]. In contrast to these findings, the perylene molecules remain mobile on the Au(1 1 0) surface until the final monolayer ($\theta = 1$ ML) is reached. The reason for this behavior is probably a weaker intermolecular van der Waals interaction of the perylene molecules compared to DMe-PTCDI and PTCDA, which have polar end groups.

A growth mode that starts with many nuclei and forms crystalline islands already in the submonolayer regime, as in the case for PTCDA and DMe-PTCDI, must lead to antiphase domain boundaries in the monolayer because above a critical size immobile islands grow together. Only below a critical size the adsorption positions of all molecules of the island may change in such a way as to be in periodic alignment with the molecular positions in adjacent islands.

In the case of perylene, there are two reasons that lead to a different monolayer growth. On the one hand the intermolecular interaction is relatively weak, which leads to a two-dimensional fluid-like behavior of the molecules in the submonolayer regime and not to island growth. On the other hand, the molecule to substrate localization is weak, i.e., the molecules are very mobile on the surface, so that adsorption positions can be aligned. Only when the coverage reaches a fully compressed monolayer (i.e. when the adsorption positions have been aligned) the molecular positions become fixed. We believe that this growth mechanism is responsible for a drastic reduction of the density of antiphase domain boundaries.

It can also be explained why antiphase domains of one specific kind still occur. In these antiphase domains, the molecular positions are aligned, but the two inequivalent positions in a unit cell are switched, i.e. the tilts of the molecules are mirrored with respect to the (0 0 1) glide plane. As the molecules are tilted as one of the last steps of the compression, to form a unit cell with two molecules, this tilting process probably starts from several points at the same time; these act as nuclei of the shown antiphase domains, with a 50:50 chance for neighboring nuclei of the final compressed structure to form an antiphase domain of this kind or not. The antiphase domain boundaries often even run along defects and step edges, since the latter are probably barriers for the tilting process of the molecules.

5. Conclusions

The structures of monolayers of perylene on Au(1 1 0) have been described. The periodicity of the missing row reconstructed Au(1 1 0) interface changes with the perylene coverage. In the order of increasing perylene density 1×4, 1×3 and 1×2 Au reconstructions appear under the perylene monolayer. The perylene molecules form $[1\,\bar{1}\,0]$-directed lines along these missing row structures. The final compressed perylene monolayer structure is a coincident one with a uniform domain

orientation. Because of their high mobility and weak interactions, the perylene molecules show a very good and long range ordering in the self-organization process. This special growth mechanism leads to a decreased density of antiphase domain boundaries as compared to systems that grow from fixed nuclei.

References

[1] J.H. Schön, Ch. Kloc, B. Batlogg, Appl. Phys. Lett. 77 (2000) 3776.
[2] W. Gebauer, M. Bässler, R. Fink, M. Sokolowsky, E. Umbach, Chem. Phys. Lett. 266 (1997) 177.
[3] W. Gebauer, C. Väterlein, A. Soukopp, M. Sokolowsky, R. Hock, H. Port, P. Bauerle, E. Umbach, Synth. Met. 87 (1997) 127.
[4] N. Karl, J. Marktanner, Mol. Cryst. Liq. Cryst. 315 (1998) 465.
[5] A.H. Schäfer, C. Seidel, H. Fuchs, Thin Solid Films 379 (2000) 176.
[6] H. Hoshi, A.J. Dann, Y. Maruyama, J. Appl. Phys. 67 (1990) 1845.
[7] C. Seidel, C. Awater, X.D. Liu, R. Ellerbrake, H. Fuchs, Surf. Sci. 371 (1997) 123.
[8] C. Seidel, A.H. Schäfer, H. Fuchs, Surf. Sci. 459 (2000) 310.
[9] C. Seidel, R. Ellerbrake, L. Gross, H. Fuchs, Phys. Rev. B, in press.
[10] Institut für PAH-Forschung, Flurstr. 17, 86926 Greifenberg am Ammersee.
[11] C. Seidel, Dissertation, Universität Stuttgart, 1993 www.kentax.de.
[12] C. Seidel, J. Poppensieker, H. Fuchs, Surf. Sci. 408 (1998) 223.
[13] F. Ercolessi, A. Bartolini, M. Garofalo, M. Parrinello, E. Tosatti, Surf. Sci. 189/190 (1987) 636.
[14] S. Speller, T. Rausch, W. Heiland, Surf. Sci. 342 (1995) 224.
[15] M. Sturmat, R. Koch, K.H. Rieder, Phys. Rev. Lett. 77 (25) (1996) 5071.
[16] T. Gritsch, D. Coulman, R.J. Behm, G. Ertl, Surf. Sci. 257 (1991) 297.
[17] M. Böhringer, W.-D. Schneider, R. Berndt, K. Glöckler, M. Sokolowski, E. Umbach, Phys. Rev. B 57 (1998) 4081.
[18] L. Gross, C. Seidel, A.H. Schäfer, H. Fuchs, Phys. Rev. B, submitted for publication.
[19] T. Schmitz-Hübsch, T. Fritz, R. Stuab, A. Back, N.R. Armstrong, K. Leo, Surf. Sci. 437 (1999) 163.